

Supporting Information for “Solar wind-magnetosphere coupling during HILDCAAs”

S. E. Milan¹*, M. K. Mooney¹, G. Bower¹, A. L. Fleetham¹, S. K. Vines²,

and J. Gjerloev²

¹Department of Physics and Astronomy, University of Leicester, Leicester, UK.

²Johns Hopkins University Applied Physics Laboratory, USA.

Contents of this file

1. Figures S1 to S12

*School of Physics and Astronomy,
University of Leicester, Leicester LE1 7RH,
UK

Introduction Figures S1 to S12 present High-Speed solar wind Stream (HSS) intervals accompanied by High-Intensity Long-Duration Continuous AE Activity (HILDCAA) to accompany the main paper. Figure S1 (Event 1 from the paper) was from the IMAGE era, whereas Figures S2 to S12 are from the AMPERE era. The latter figures are presented in the same format as Figure 3. Figure S1 is presented in a slightly modified form, in which panel (e) shows the polar cap or open flux, F_{PC} , quantified from observations of the auroral oval by IMAGE.

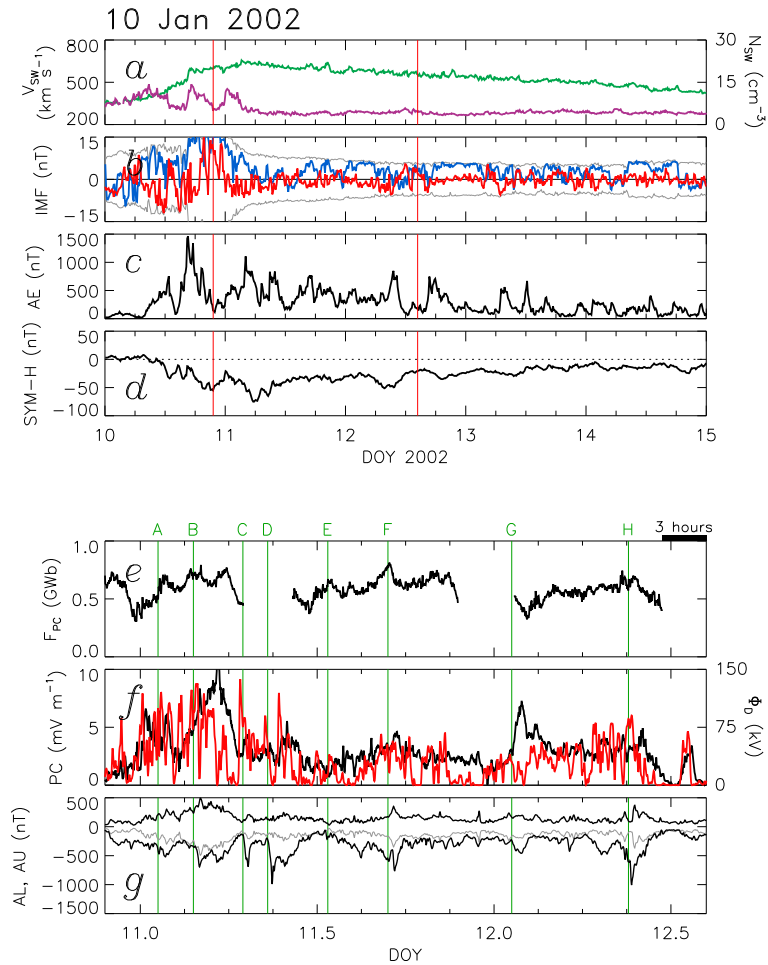


Figure S1. Solar wind and magnetospheric parameters during Event 1. (a) Solar wind speed (green) and number density (purple); (b) the B_Y (blue) and B_Z (red) components of the IMF, and the IMF magnitude (grey); (c) the AE index; (d) the Sym-H index. Vertical red lines delineate the period shown in the lower panels. (e) F_{PC} quantified from observations of the auroral oval by IMAGE; (f) The PC index (black) and Φ_D^* (red); (g) the AU and AL indices.

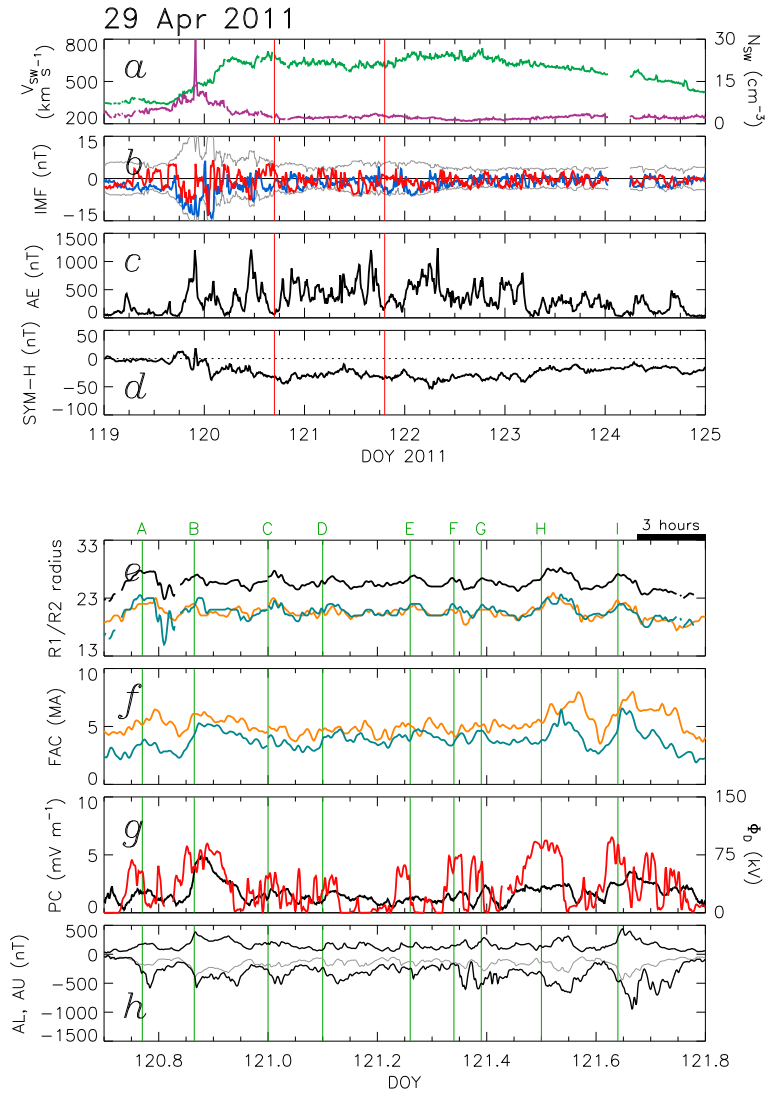


Figure S2. Solar wind and magnetospheric parameters during Event 2. (a) Solar wind speed (green) and number density (purple); (b) the B_Y (blue) and B_Z (red) components of the IMF, and the IMF magnitude (grey); (c) the AE index; (d) the Sym-H index. Vertical red lines delineate the period shown in the lower panels. (e) The radius of the boundary between the R1 and R2 FACs, Λ° , in the northern (black) and southern (blue) hemispheres, quantified from observations of the FACs by AMPERE; the average is shown in black, offset by $+5^\circ$ for clarity. (f) The northern (orange) and southern (blue) hemispherically-integrated FACs; (g) The PC index (black) and Φ_D^* (red); (h) the AU and AL indices.

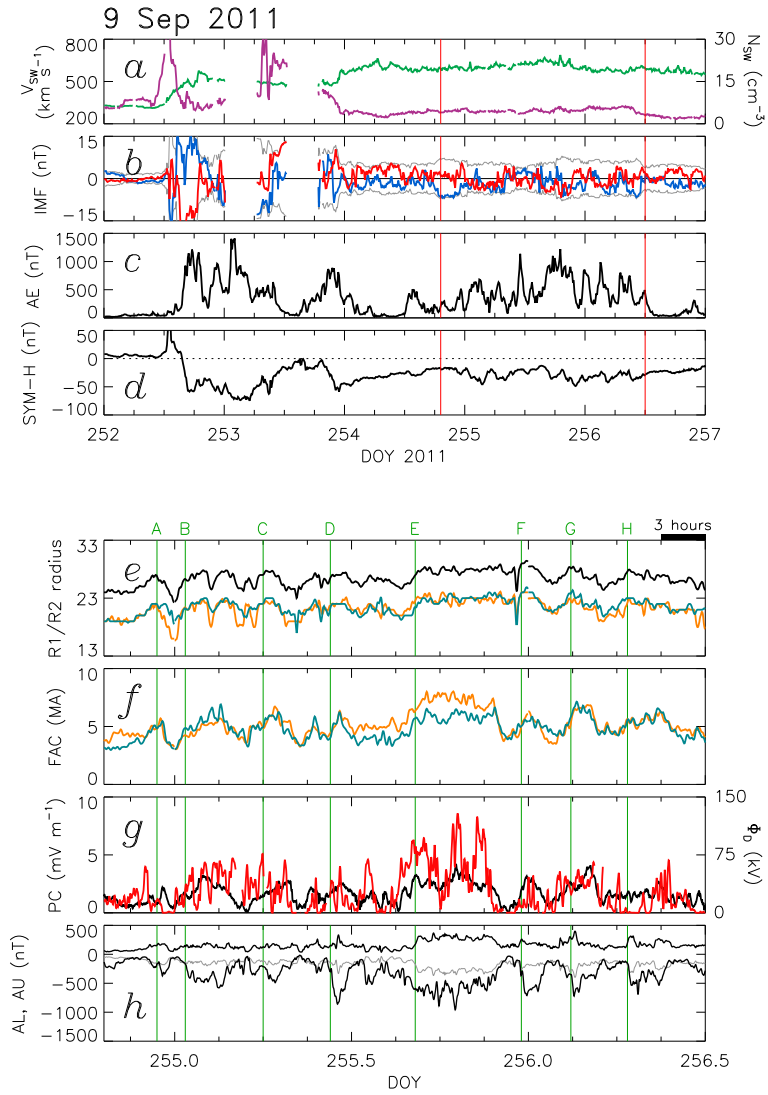


Figure S3. Solar wind and magnetospheric parameters during Event 3, presented in the same format as Figure S2.

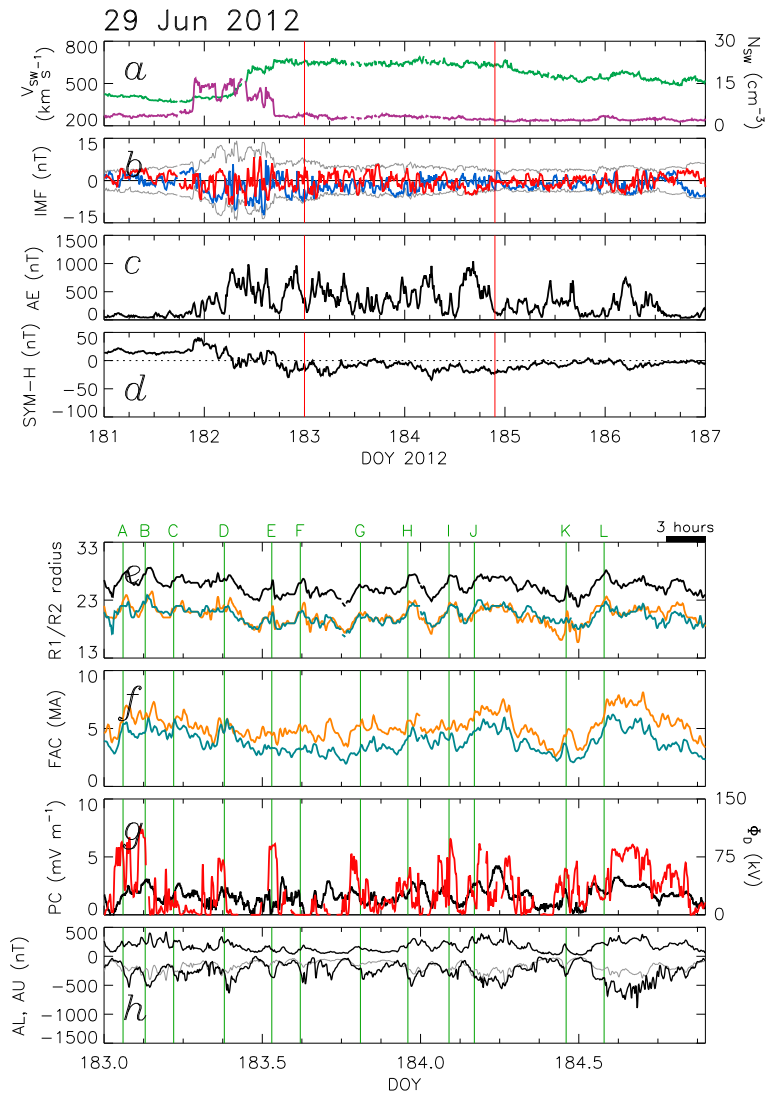


Figure S4. Solar wind and magnetospheric parameters during Event 5, presented in the same format as Figure S2.

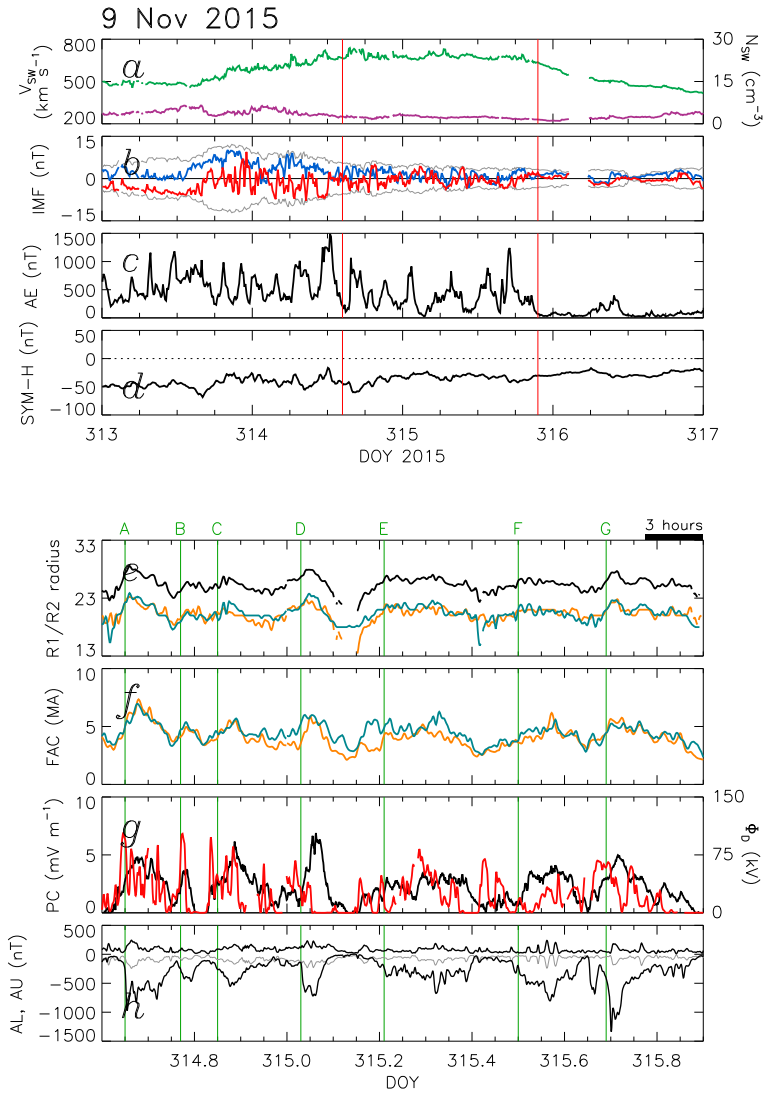


Figure S5. Solar wind and magnetospheric parameters during Event 7, presented in the same format as Figure S2.

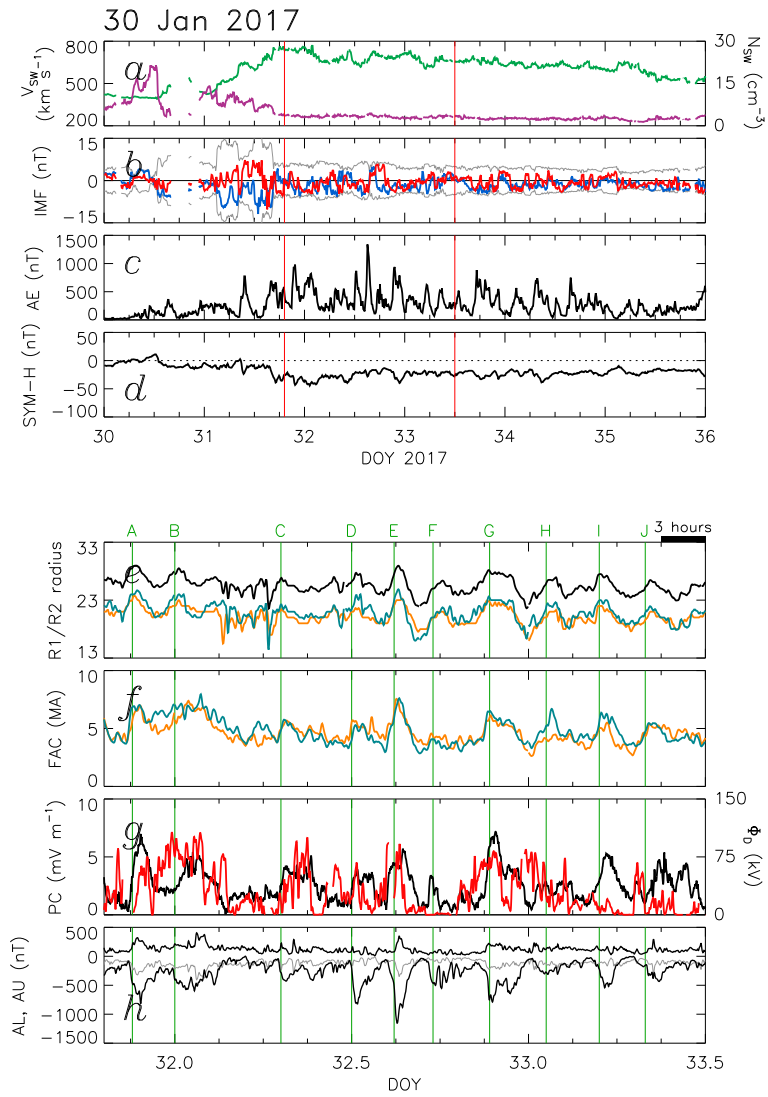


Figure S6. Solar wind and magnetospheric parameters during Event 9, presented in the same format as Figure S2.

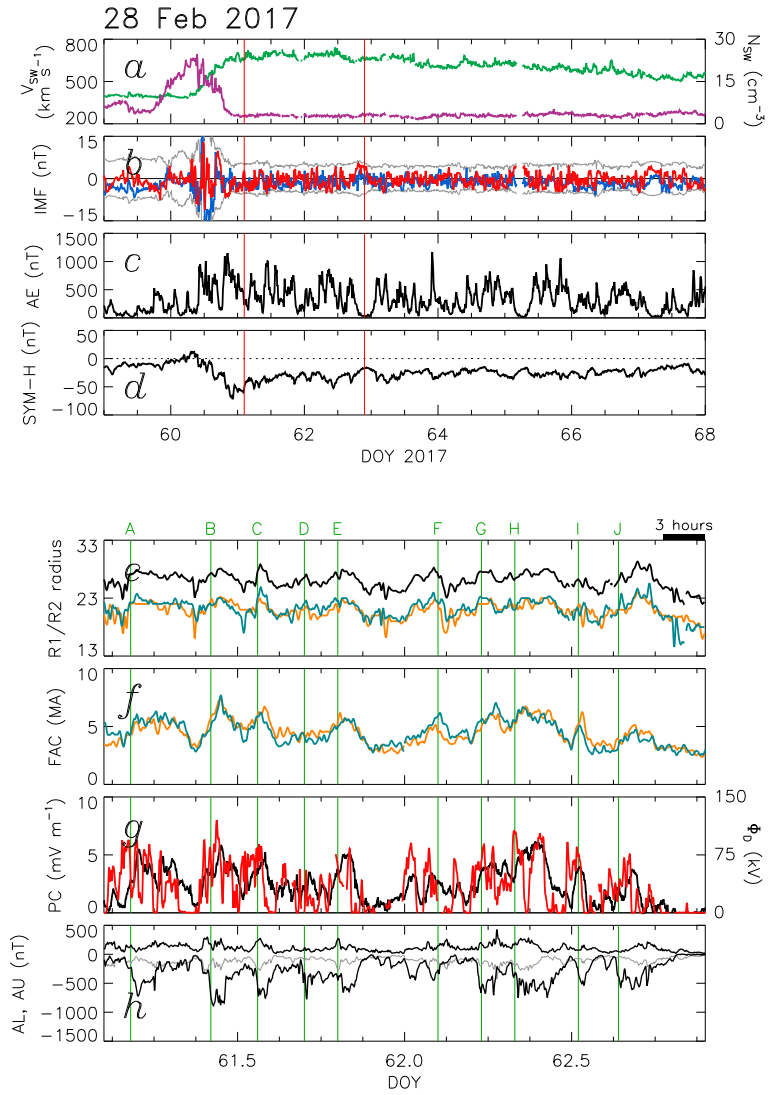


Figure S7. Solar wind and magnetospheric parameters during Event 10, presented in the same format as Figure S2.

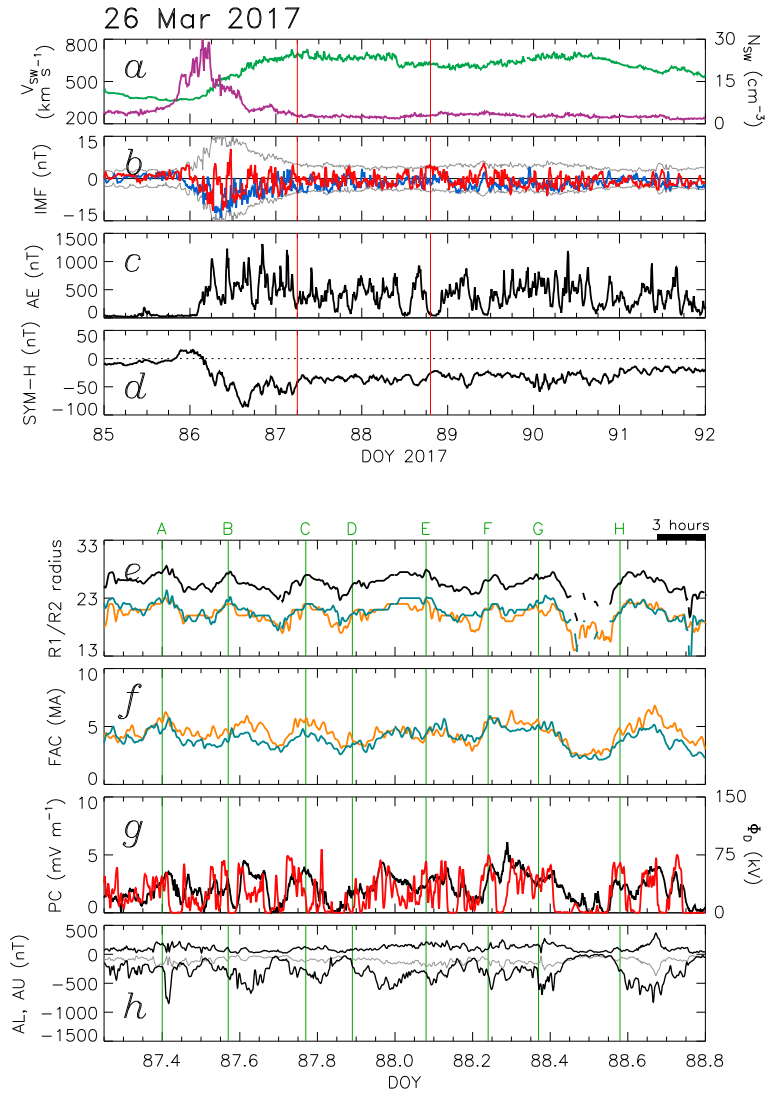


Figure S8. Solar wind and magnetospheric parameters during Event 11, presented in the same format as Figure S2.

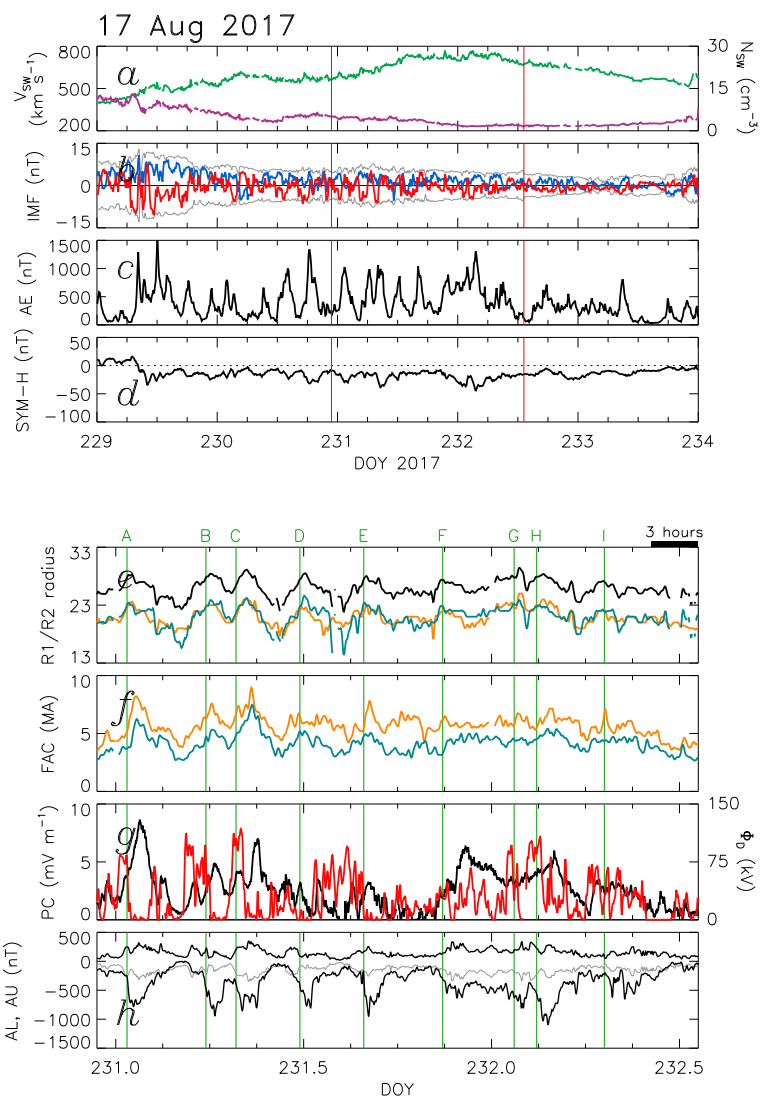


Figure S9. Solar wind and magnetospheric parameters during Event 13, presented in the same format as Figure S2.

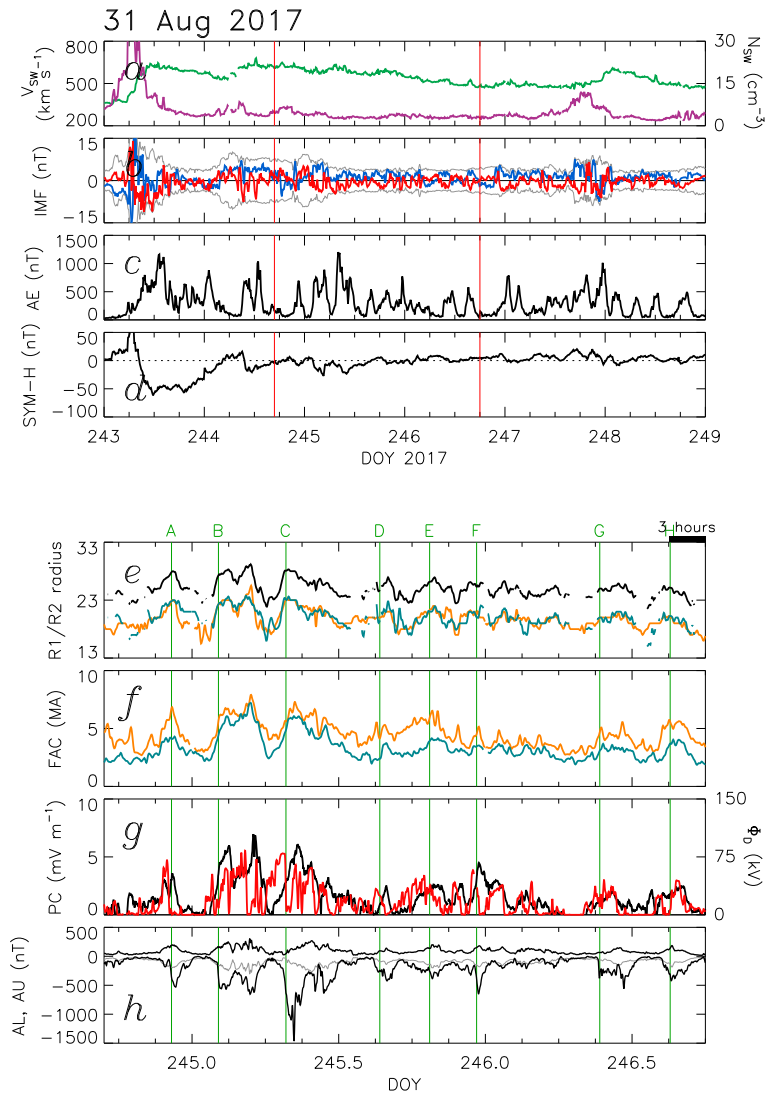


Figure S10. Solar wind and magnetospheric parameters during Event 14, presented in the same format as Figure S2.

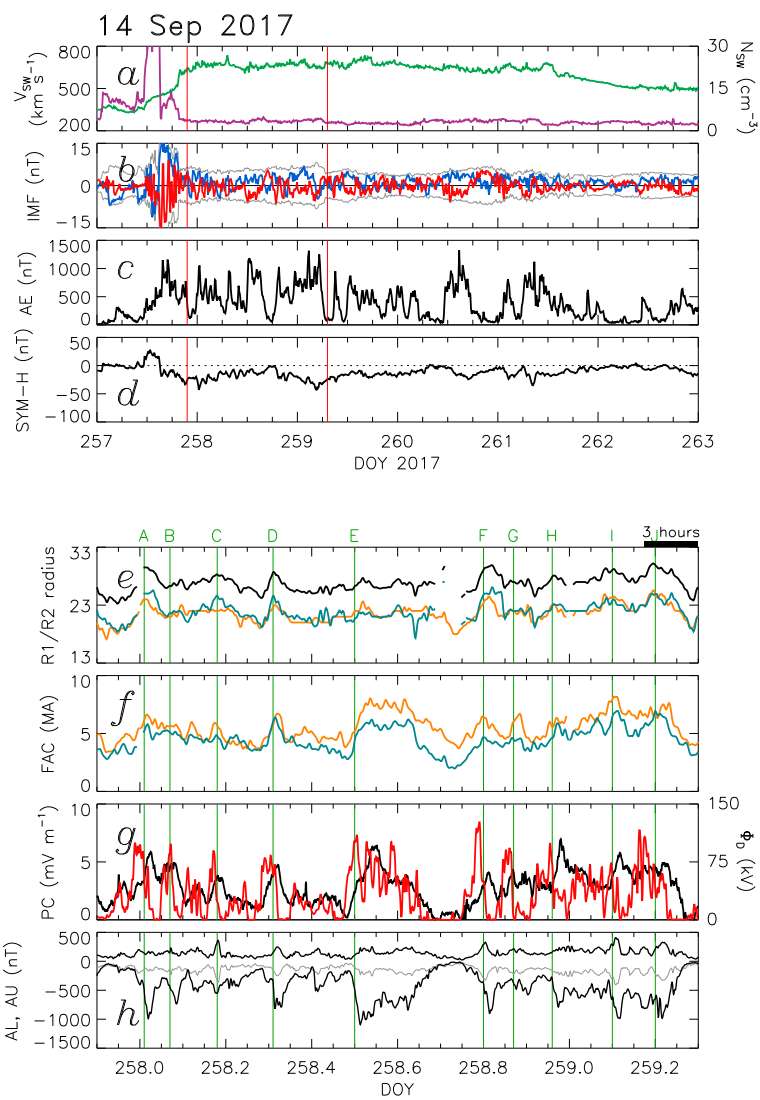


Figure S11. Solar wind and magnetospheric parameters during Event 15, presented in the same format as Figure S2.

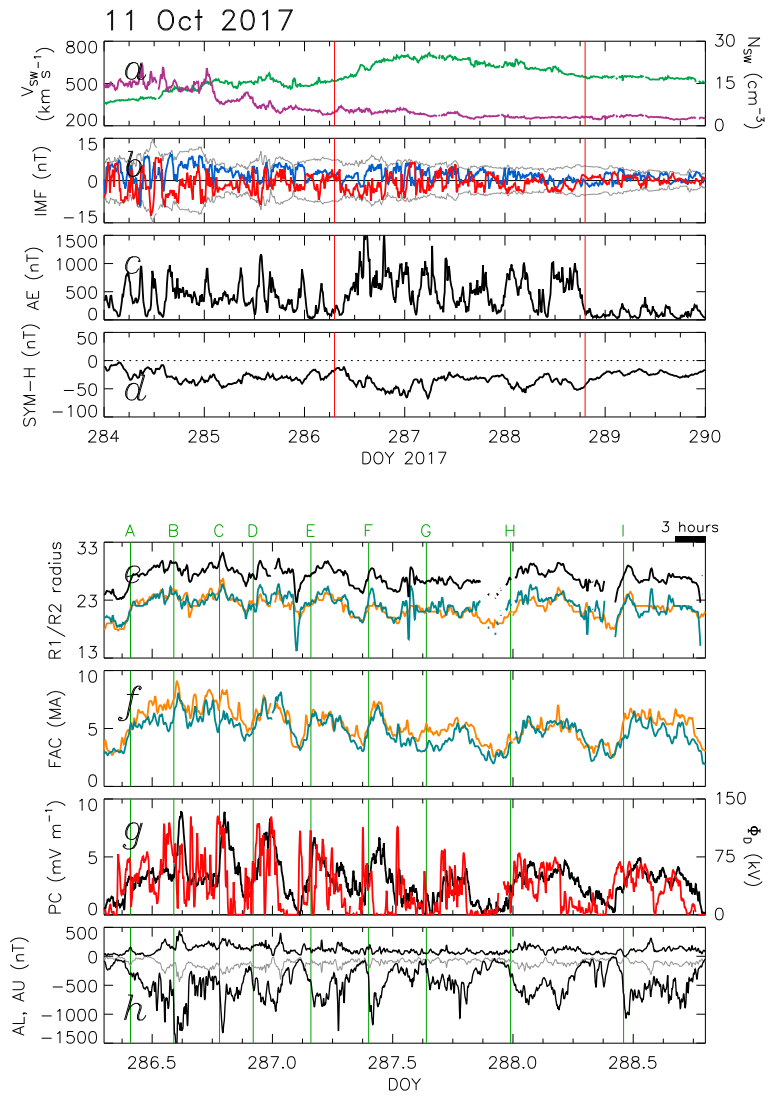


Figure S12. Solar wind and magnetospheric parameters during Event 16, presented in the same format as Figure S2.